

Using H_∞ Control Theory Designing of Robust UPFC Controller in Power System

¹Kanika Goel, ²Snigdha Sharma, ³Anmol Gupta, ⁴Gurpreet Singh

¹Faculty (IAMR College of Engineering, Meerut, kanikagoel31@gmail.com)

²Faculty (Shanti Institute of Technology, Meerut, sniky.2206@gmail.com)

³Assistant Professor & Head (IAMR College of Engineering, Meerut, anmol.engg@gmail.com)

⁴Assistant Prof. (Ideal Institute of Technology, Ghaziabad, gurpreet24@gmail.com)

ABSTRACT

A power system always contains parametric uncertainties. In the design of a controller the uncertainties have to be considered. Otherwise, if the real plant differs from the assumed plant model, a controller, designed based on classical controller design approaches, may not ensure the stability of the overall system. In this paper design of robust control for the UPFC controllers including power flow and DC voltage regulator, using a H_∞ loop-shaping design via a normalized co prime factorization approach, where loop-shape refers to magnitude of the loop transfer function $L = GK$ as function of frequency is presented. As an example, we have designed a case for the system to compare the proposed method with a conventional method (classical P-I controller). AS the results of the linear and nonlinear simulations, the validity of the proposed method has been confirmed.

Key words: Flexible AC transmission system (FACTS); H_∞ loop shaping; Power system Oscillation; Unified power flow controller (UPFC).

I. INTRODUCTION

The Flexible AC Transmission Systems (FACTS) based on power electronics offer an opportunity to enhance controllability, stability, and power transfer capability of AC transmission systems [1]. The Unified Power Flow Controller (UPFC), which is the most versatile FACTS device, has the capabilities of controlling power flow in the transmission line, improving the transient stability, mitigating system oscillation and providing voltage support[2-4]. PID is the most commonly used control algorithm in the process industry. Also, this technique is used to control the FACTS devices [5]. However, the nonlinear nature of well as the uncertainties that exist in the system make it difficult to design an effective controller for the FACTS that guarantees fast and stable regulation under all operating conditions. A major source of difficulty is that open-loop plant may change. In particular, inaccuracy in plant may cause problems because the plant is part of the feedback loop. To deal with such a problem, instead of using a single model plant, an uncertain model should be considered. This problem has led to the study of applying adaptive controllers for instance [6, 7], nonlinear controllers for instance [8] in the power system stability control. Also, during past decade, the H_∞ optimal robust control design has received increasing attention in power systems. Most of above methods have been applied in power systems and some of these efforts have contributed to the design of supplementary control for SVC using mixed sensitivity[9], applying μ -synthesis for SVC in order to voltage control design[10] and supplementary control design for SVC and STATCOM[11]. For many control problems, a design procedure is required that offers more flexibility than mixed sensitivity, but should not be as complicated as μ -synthesis and should not be limited in its application like LTR procedures. The H_∞ loop-shaping design is such a controller procedure, used to design a robust controller for FACTS control to improve the system damping [12].

In this paper as an example, a Single Machine Infinite Bus (SMIB) power system installed with a UPFC is considered for case study and H_∞ loop-shaping method is used to design a robust controller for UPFC controller including power-flow and DC-voltage regulator in this system. To show influence of proposed method, the proposed method is compared to conventional method (the parameters of conventional P-I controller are

optimized using genetic algorithm).As the validity of the proposed method has been confirmed by linear and nonlinear time domain simulation results.

II. MATERIALS AND METHODS

Figure 1 shows a SMIB system equipped with a UPFC.

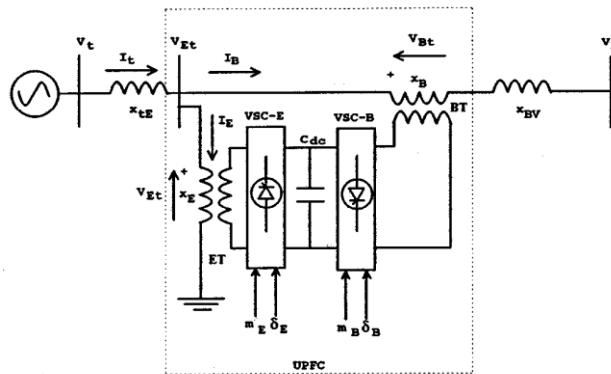


Fig. 1: SMIB power system equipped with UPFC

The UPFC consists of an Excitation Transformer (ET), a Boosting Transformer (BT), two three-phase GTO based voltage source converters (VSCs) and a DC link capacitors. The four input control signals to the UPFC are m_E , m_B , δ_E , and δ_B , where, m_E is the excitation amplitude modulation ratio, m_B is the boosting amplitude modulation ratio, δ_E is the excitation phase angle and δ_B is the boosting phase angle.

(i) **Non-Linear Dynamic Model:** By applying Park’s transformation and neglecting the resistance and transients of the ET and BT transformers, the UPFC can be modeled as [13-15]:

$$\begin{bmatrix} v_{Et d} \\ v_{Et q} \end{bmatrix} = \begin{bmatrix} 0 & -x_E \\ x_E & 0 \end{bmatrix} \begin{bmatrix} i_{E d} \\ i_{E q} \end{bmatrix} + \begin{bmatrix} \frac{m_E \cos \delta_E v_{dc}}{2} \\ \frac{m_E \sin \delta_E v_{dc}}{2} \end{bmatrix} \quad (1)$$

$$\begin{bmatrix} v_{Bt d} \\ v_{Bt q} \end{bmatrix} = \begin{bmatrix} 0 & -x_B \\ x_B & 0 \end{bmatrix} \begin{bmatrix} i_{B d} \\ i_{B q} \end{bmatrix} + \begin{bmatrix} \frac{m_B \cos \delta_B v_{dc}}{2} \\ \frac{m_B \sin \delta_B v_{dc}}{2} \end{bmatrix} \quad (2)$$

$$\frac{dv_{dc}}{dt} = \frac{3m_E}{4C_{dc}} [\cos \delta_E \quad \sin \delta_E] \begin{bmatrix} i_{E d} \\ i_{E q} \end{bmatrix} + \frac{3m_B}{4C_{dc}} [\cos \delta_B \quad \sin \delta_B] \begin{bmatrix} i_{B d} \\ i_{B q} \end{bmatrix} \quad (3)$$

Where, V_{ET} , i_E , V_{BT} and i_B are the excitation voltage, excitation current, boosting voltage, and boosting current, respectively; C_{dc} and V_{dc} are the DC link capacitance and voltage, respectively. The nonlinear model of the SMIB system as shown in Fig. 1 is described by:

$$\dot{\delta} = \omega_o \omega \quad (4)$$

$$\dot{\omega} = \frac{(P_m - P_e - D\omega)}{M} \quad (5)$$

$$E_q' = \frac{(-E_q + E_{fd})}{T_{do}'} \quad (6)$$

$$E'_{fd} = \frac{-1}{T_A} E_{fd} + \frac{K_A}{T_A} (V_{to} - V_t) \quad (7)$$

Where,

$$T_e = P_e = v_{qt} i_{qt} + v_{dt} i_{dt}$$

$$E_q = E'_q + (x_d - x'_d) i_{dt}$$

$$E_q = E'_q - x'_d i_{dt}$$

$$v_{dt} = x_q i_{qt}$$

$$v_t = \sqrt{v_{dt}^2 + v_{qt}^2}$$

$$i_{dt} = i_{Ed} + i_{Bd}$$

$$i_{qt} = i_{Eq} + i_{Bq}$$

$$V_t = jx_{te} I_t + V_{Et}$$

$$V_{Et} = V_{Bt} + jx_{BV} I_B + V_b$$

$$\begin{bmatrix} i_{Eq} \\ i_{Bq} \end{bmatrix} = \begin{bmatrix} x_q + x_{tE} + x_E & x_q + x_{tE} \\ x_E & -x_B - x_{BV} \end{bmatrix}^{-1} \begin{bmatrix} \frac{m_E \cos \delta_E v_{dc}}{2} \\ \frac{m_E \cos \delta_E v_{dc}}{2} - \frac{m_B \cos \delta_B v_{dc}}{2} - V_b \sin \delta \end{bmatrix}$$

$$\begin{bmatrix} i_{Ed} \\ i_{Bd} \end{bmatrix} = \begin{bmatrix} x'_d + x_{tE} + x_E & x'_d + x_{tE} \\ x_E & -x_B - x_{BV} \end{bmatrix}^{-1} \begin{bmatrix} E'_q - \frac{m_E \sin \delta_E v_{dc}}{2} \\ \frac{m_B \sin \delta_B v_{dc}}{2} - \frac{m_E \cos \delta_E v_{dc}}{2} - V_b \cos \delta \end{bmatrix}$$

$$X_{qt} = X_q + X_{tE} + X_E$$

$$X_{qE} = X_q + X_{tE}$$

$$X_{dt} = X_E + X'_d + X_{tE}$$

$$X_{dE} = X'_d + X_{tE}$$

$$X_{BB} = X_B + X_{BV}$$

$$X_{qE} = X_{qt} X_{BB} + X_E X_{qE}$$

$$X_{dE} = -X_{dt} X_{BB} - X_{dE} X_E$$

$$X_{Bd} = X_B + X_{BV} + X'_d + X_{tE}$$

$$X_{Bq} = X_B + X_{BV} + X_q + X_{tE}$$

(ii) **Power system linearised model:** A linear dynamic model is obtained by linearising the nonlinear model round an operating condition. The linearised model of power system as shown in Fig. 1 is given as follows:

$$\dot{\delta} = \omega_o \Delta \omega \quad (8)$$

$$\Delta \dot{\omega} = \frac{(P_m - P_e - D \Delta \omega)}{2H} \quad (9)$$

$$E'_q = \frac{(-E_q + E_{qe})}{T_{do}'} \quad (10)$$

$$E'_{qs} = \text{Reg}(s)(V_{to} - V_t) = \frac{K_A(V_{to} - V_t)}{1 + sT_A} \quad (11)$$

Where

$$P_s = \frac{E_q' V_b \sin \delta}{X_{d\Sigma}'} - \frac{V_b^2 (X_q - X_d') \sin 2\delta}{2X_{d\Sigma}' X_{d\Sigma}'}$$

$$E_q = \frac{X_{d\Sigma}' E_q'}{X_{d\Sigma}'} - \frac{(X_d - X_d') V_b \cos \delta}{X_{d\Sigma}'}$$

$$V_{td} = \frac{X_q V_b \sin \delta}{X_{d\Sigma}'}$$

$$V_{tq} = \frac{X_L E_q'}{X_{d\Sigma}'} + \frac{V_b X_d' \cos \delta}{X_{d\Sigma}'}$$

$$X'_{d\Sigma} = X'_d + X_L$$

$$X_{q\Sigma} = X_q + X_L$$

$$X_{d\Sigma} = X_d + X_L$$

By linearizing equations we obtain the state variable equation of power system installed with the UPFC to be

$$\begin{bmatrix} \Delta \delta \\ \Delta \omega \\ \Delta E'_q \\ \Delta E'_{fd} \end{bmatrix} = \begin{bmatrix} 0 & \omega_o & 0 & 0 \\ -\frac{K_1}{M} & -D & -\frac{K_2}{M} & 0 \\ -\frac{K_4}{T_{do}'} & 0 & -\frac{K_3}{T_{do}'} & \frac{1}{T_{do}'} \\ -\frac{K_A K_E}{T_A} & 0 & -\frac{K_A K_E}{T_A} & -\frac{1}{T_A} \end{bmatrix} \begin{bmatrix} \Delta \delta \\ \Delta \omega \\ \Delta E'_q \\ \Delta E'_{fd} \end{bmatrix} + \begin{bmatrix} 0 \\ -\frac{K_{pd}}{M} \\ -\frac{K_{qd}}{T_{do}'} \\ -\frac{K_A K_{vd}}{T_A} \end{bmatrix} \Delta v_{dc} + \begin{bmatrix} 0 & 0 & 0 & 0 \\ -\frac{K_{pe}}{M} & -\frac{K_{p\delta e}}{M} & -\frac{K_{pb}}{M} & -\frac{K_{p\delta b}}{M} \\ -\frac{K_{qe}}{T_{do}'} & -\frac{K_{q\delta e}}{T_{do}'} & -\frac{K_{qb}}{T_{do}'} & -\frac{K_{q\delta b}}{T_{do}'} \\ -\frac{K_A K_{ve}}{T_A} & -\frac{K_A K_{v\delta e}}{T_A} & -\frac{K_A K_{vb}}{T_A} & -\frac{K_A K_{v\delta b}}{T_A} \end{bmatrix} \begin{bmatrix} \Delta m_E \\ \Delta m_B \\ \Delta \delta_E \\ \Delta \delta_B \end{bmatrix} \quad (12)$$

Where $\Delta m_E, \Delta m_B, \Delta \delta_E, \Delta \delta_B$ are the deviation of input control signals to the UPFC and Δv_{dc} is that of DC bus voltage between the two converters.

The linearized model of the power system installed with the UPFC can also be drawn with following parameters

$$\Delta f_s = [\Delta v_{dc} \quad \Delta u_k]$$

$$K_p = \begin{bmatrix} \frac{K_{pd}}{M} \\ \frac{K_{puk}}{M} \end{bmatrix}, \quad K_q = \begin{bmatrix} \frac{K_{qd}}{T_{do}'} \\ \frac{K_{quk}}{T_{do}'} \end{bmatrix}, \quad K_v = \begin{bmatrix} \frac{K_A K_{vd}}{T_A T_{do}'} \\ \frac{K_A K_{vuk}}{T_A T_{do}'} \end{bmatrix}$$

If the input control signal to the UPFC, which is selected to be superimposed by the control output of the UPFC based stabilizer is Δu_k , then e , b , δ_e and δ_b imply that $\Delta u_k = \Delta m_E$, $\Delta u_k = \Delta m_B$, $\Delta u_k = \Delta \delta_E$ or $\Delta u_k = \Delta \delta_B$ respectively. The block diagram of the linearised dynamic model of the SMIB power system with UPFC is shown in Fig. 2.

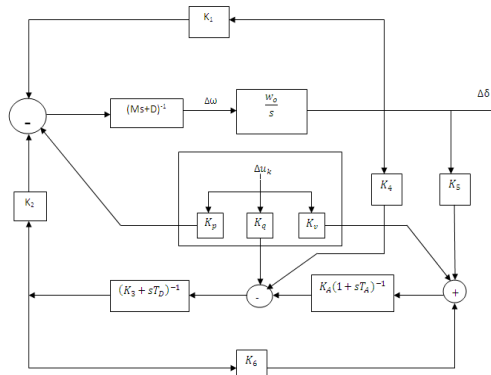


Fig. 2: Linearised dynamic model of the SMIB power system with UPFC

(iii) **H_∞ Loop-shaping design:** The adopted control method is based on H_∞ robust stabilization combined with classical Loop-shaping, where loop-shape refers to the magnitude of the loop transfer function $L = GK$ as a function of frequency. It is essentially a tow-step procedure, where in the first step; the singular values of the open-loop plant are shaped by pre and post compensators. In the second step, the resulting shaped plant is robustly stabilized with respect to coprime factor uncertainty using H_∞ optimization. An important advantage is that no problem-dependent uncertainty modelling, or weight selection, is required in this second step [16]. The stabilization of the plant G has a normalized left co-prime factorization given by:

$$G = M^{-1}N \tag{13}$$

A perturbed plant model G_Δ can then be written as:

$$G_\Delta = (M_s + \Delta M_s)^{-1}(N_s + \Delta N_s) \tag{14}$$

The objective of the robust stabilization is to stabilize not only the nominal model G_Δ but also the perturbed model given as:

$$G_\Delta = \{(M_s + \Delta M_s)^{-1}(N_s + \Delta N_s) : \|\Delta N_s \Delta M_s\| \leq 1/\gamma\} \tag{15}$$

Where ΔM_s and ΔN_s are stable unknown transfer functions which represent system uncertainty in the nominal plant model.

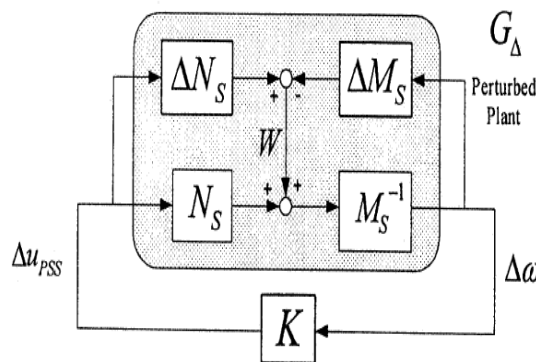


Fig. 3: H_∞ robust stabilization problem

For the perturbed feedback system of Fig. 3, the stability property is Robust if and only if, the nominal feedback system is stable and:

$$\left\| \begin{bmatrix} I \\ K_\infty \end{bmatrix} (I - G_s K_\infty)^{-1} M_s^{-1} \right\|_\infty \leq \epsilon^{-1} \quad (16)$$

The lowest achievable value of γ and corresponding maximum stability margin ϵ are given by:

$$\gamma_{min} = \sqrt{1 + \lambda_{max}(XZ)} \quad (17)$$

Where $\|\cdot\|_\infty$ denotes the Hankel norm and for a minimal state space realization (A, B, C, D) of G, Z and X are the unique positive definite solution to the algebraic Riccati equations:

$$(A - BS^{-1}D^T C)^T X + X(A - BS^{-1}D^T C) - XBS^{-1}B^T X + C^T R^{-1}C = 0 \quad (18)$$

$$(A - BS^{-1}D^T C)Z + Z(A - BS^{-1}D^T C)^T - ZC^T R^{-1}CZ + BS^{-1}B^T = 0 \quad (19)$$

Where $R = I + DD^T$, and $S = I + D^T D$.

For a specified $\gamma > \gamma_{min}$ is given by:

$$K_\infty = \begin{bmatrix} A + BF + \gamma^2(L^T)^{-1}ZC^T(C + DF) & \gamma^2(L^T)^{-1}ZC^T \\ B^T X & -D^T \end{bmatrix} \quad (20)$$

Where $F = -S^{-1}(D^T C + B^T X)$ and $L = (1 - \gamma^2)I + XZ$.

It is important to emphasize that, since γ_{min} is computed from (19) and an explicit solution has been derived by solving just two Riccati equations and the γ iteration needed to solve them, the general H_∞ problem has been avoided [16-17].

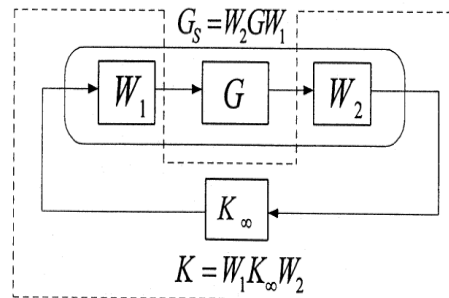


Fig. 4: shaped plant and controller

The controller design procedure can be summarized as follows.

(iv) **Loop Shaping:** Using pre- and post compensators W_1 and W_2 , the singular values of the plant are shaped to give a desired open loop shape as shown in Fig. 4.

Some trial and error is involved Here W_2 is usually chosen as a constant. W_1 contains dynamic shaping.

Integral action for low frequency performance, phase advance for reducing the roll-off rates at crossover, and phase-lag to increase the roll-off rates at high frequencies, should all be placed in W_1 if desired. The weights should be chosen so that no unstable hidden modes are created in G_s .

(v) **Robust Stabilization:** Robustly stabilize the shaped plant G_s . First, calculate the maximum stability margin $\epsilon_{max} < 1/\gamma_{min}$. If the margin is too small, $\epsilon_{max} < 0.25$, return to step 1 and adjust the weight. Otherwise, select $\gamma > \gamma_{min}$ by about 10% and synthesis a suboptimal controller using (22). When $\epsilon_{max} > 0.25$ (respectively, $\gamma_{min} < 4$) the design is usually successful. A small value of ϵ_{max} indicates that the chosen singular value loop

shapes are incompatible with robust stability requirements. The loop shape does not change much following robust stabilization if y is small [16-17]

If all the specification is not met: Return to step 1 and make further modification to the weights.

Reduce the order of controller: Check the frequency response plot of K_{s-red} against that of K_s .

Final feedback controller K : This is achieved by combining K_{s-red} with the shaping function W_1 and W_2 such that $K = W_1 K_{s-red} W_2$.

III. CONTROLLER DESIGN USING H_∞ THEORY

Due to system parameters are given in Appendix, the initial d-q axes voltage, current components and torque angle are computed for the nominal operating condition as follows:

$$\begin{aligned} \delta_o &= 47.1477^\circ \\ E_{bdo} &= 0.7331 \text{ pu} & E_{bqo} &= 0.6801 \text{ pu} \\ e_{do} &= 0.3999 \text{ pu} & e_{qo} &= 0.9165 \text{ pu} \\ i_{do} &= 0.4728 \text{ pu} & i_{qo} &= 0.6665 \text{ pu} \end{aligned}$$

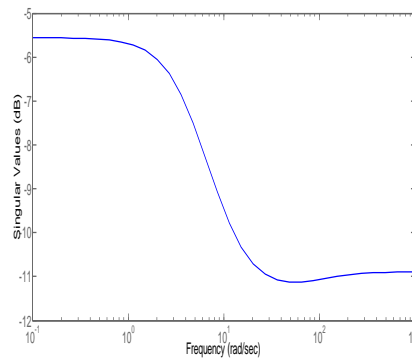


Fig. 5: Singular values of open loop of DC voltage regulator

(i) **Design of UPFC controller:** The UPFC power-flow and DC voltage regulator are designed independently. The following controller design results are obtained. First, the singular values of the open loop are calculated. After trial and error, W_1 and W_2 for power flow controller are chosen:

$$W_1 = \frac{14.8(s + 0.515)}{s(s + 10)(s + 0.1647)} \quad W_2 = 1$$

The variable (γ_{min}) is the inverse of the magnitude of coprime uncertainty, which can be tolerated before getting instability. $\gamma_{min} > 1$ should be as small as possible, and usually requires that γ_{min} is less than a value of 4 [16-17]. By applying this, $\gamma_{min} = 1.7137$ for power flow controller are obtained. In order to show influence of H_∞ loop-shaping method, the proposed method is compared to conventional method. In conventional method, the parameters of the power-flow controller (k_{pp} and k_{pi}) are optimized using genetic algorithm [20]. Optimum values of the proportional and integral gain settings of the power-flow controller are obtained as $k_{pp} = 2$ and $k_{pi} = 0.35$.

Using a commercially available software package [21], two controllers satisfying design objectives are obtained. For easy implementation, the order has been reduced by model reduction technique. The transfer functions of the controller are:

$$K_{red}(s) = \frac{0.02s^4 + 20.63s^3 + 118.3s^2 + 88.21s + 16.87}{s^5 + 16.98s^4 + 73.58s^3 + 42.46s^2 + 5.073s}$$

(ii) **Design of PSS:** The damping controllers are designed to produce an electrical torque in phase with the speed deviation according to phase compensation method.

The four control parameters of the UPFC (mB , mE , δB and δE) can be modulated in order to produce the damping torque. In this paper mB is modulated in order to damping controller design. The speed deviation is considered as the input to the damping controllers. It consists of gain, signal washout and phase compensator blocks. The parameters of the damping controller are obtained using the phase compensation technique. The detailed Step-by-step procedure for computing the parameters of the damping controllers using phase compensation technique is given [16, 17].

Damping controller mB was designed and obtained as follows (wash-out block is considered).

IV. RESULTS AND DISCUSSION

In order to examine the robustness of the UPFC power-flow controller in the presence of wide variation in loading condition, the system load is varied over a wide range.

Dynamic responses are obtained for the following three conditions:

Case 1: $\Delta T_m = 0.01$ pu,

Case 2: $\Delta T_m = 0.05$ pu,

Case 3: $\Delta T_m = 0.1$ pu.

The performance of the designed H_∞ -UPFC and classic-UPFC controllers with damping controller mB after sudden change in reference power on transmission line 2. The proposed controller designed (H_∞ -UPFC) significantly damp power system oscillations compared to conventional (classical P-I) UPFC controllers (C-UPFC). In order to investigate the performance of the proposed controller and the system behaviour under large disturbances and various operating conditions, a transitory 3-phase fault of 5-10 ms duration at the generator terminals is considered. Dynamic performance is obtained using the non-linear model under the system of the nominal and heavy loading condition with H_∞ -based and optimal settings of the UPFC controllers (Power-flow controller and damping controller). The proposed controller designed significantly damp power system oscillations compared to conventional (classical P-I) UPFC controllers (C-UPFC).

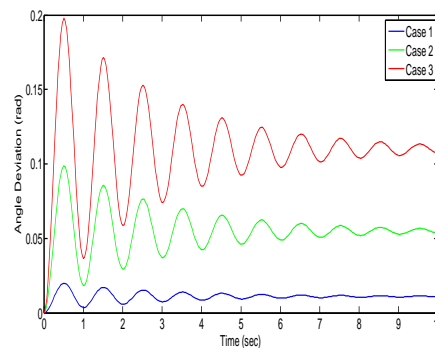


Fig.6: Dynamic responses for all three cases for SMIB system without UPFC

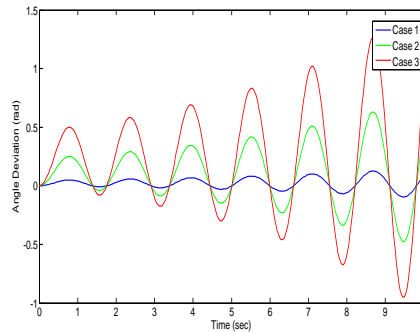


Fig.7: Dynamic responses for all three cases for SMIB system with UPFC

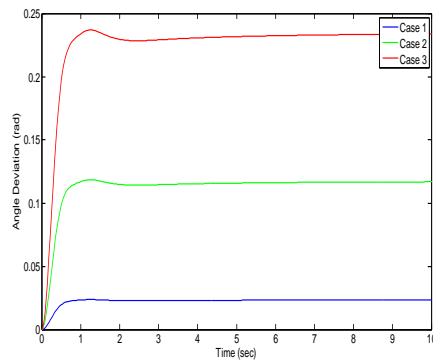


Fig.8: Dynamic responses for all three cases for SMIB system using Robust damping controller for UPFC

V. CONCLUSION

In this paper, the design of robust controller based on H_∞ theory with application to an UPFC has been carried out for power system. The performance of the controller has been evaluated in comparison with conventional UPFC by linear and nonlinear time domain simulations. The following issues have been addressed:

- 1) representation of non-linear characteristics of the system by uncertainty model principle
- 2) selection of appropriate weighting functions based on the control system objectives
- 3) Verification of the H_∞ controller design by time domain simulations under various operating conditions.

The main conclusions are:

- The robust controller can improve the damping of power system oscillation.
- The non-linear characteristics of the system can easily be incorporated into the controller design by suitable selection of weighting functions.
- The results of these studies show that the proposed controller design using H_∞ method compared to conventional method, has an excellent capability in damping of power system oscillations.
- Performance of damping controllers under large perturbations show the superiority of proposed H_∞ -based controller over its conventional counterpart. Also, effectiveness of the proposed control strategy in damping the local low frequency oscillations with UPFC is confirmed.

VI. APPENDIX

The nominal parameters and operating condition of the system are given below:

Generator: $M = 8 \text{ MJ/MVA}$ $T'do=5.044s$ $Sd = 1 \text{ pu or sec}$ $D = 0$
 $Xq = 0.6 \text{ pu}$ $X'd = 0.3 \text{ pu}$
 Excitation system: $Ka= 100$ $Ta= 0.01 \text{ sec}$

Transformers: $X_{IE} = 0.1$ pu $X_E = 0.1$ pu
 $X_B = 0.1$ pu
 Transmission line: $X_{T1} = 0.3$ pu, $X_{T2} = 0.5$ pu
 Operating condition: $P = 0.8$ pu $Q = 0.15$ pu
 $V_t = 1.0$ pu
 DC link parameter: $V_{DC} = 2$ pu $C_{DC} = 1$ pu
 UPFC parameter: $m_B = 0.0789$ pu $\delta_B = -78.21^\circ$
 $m_E = 0.4013$ pu $\delta_E = -85.34^\circ$

VII. REFERENCES

- [1] Hingorani N.G. and L. Gyugui, 2000. Understanding FACTS, IEEE Press, New York.
- [2] Gyugyi L. and C.D. Schauder, 1995. The unified power flow controller: a new approach to power transmission control, *IEEE Trans. Power Deliv.*, 10(2): 1085-1093.
- [3] Gyugyi L., 1992, Unified power flow control concept for flexible ac transmission systems, *IEEE Proceedings-C*, 139(4): 323-331.
- [4] Al-Awami A.T., Y.L. Abdel-Magid and M.A. Abido, 2007. A Particle-Swarm-Based Approach of Power System Stability Enhancement with UPFC, *Elect. Power and Energy Systems*, 29: 251-259.
- [5] Liou K.L. and Y.Y. Hsu, 1986. Damping of generator oscillation using svc, *IEEE Trans. Aero. Electron. Sys.*, 22(5): 605-617.
- [6] Liou K.L. and Y.Y. Hsu, 1992. Damping of generator oscillation using an adaptive static var compensator, *IEEE Trans. Power Deliv.*, 7(2): 718-725.
- [7] Smith J.R., D.A. Pierre, A.D. Rudberg, I. Sadighi and A.P. Johnson, 1989. An enhanced lq adaptive var unit controller for power system damping, *IEEE Trans. Power Deliv.*, 4(2): 443-451.
- [8] Ni Y., L. Jiao, S. Chen and B. Zhang, 1998. Application of a nonlinear pid controller on statcom with a differential tracker, *International Conference on Energy Management and Power Delivery, EMPD-98*, New York: 29-34.
- [9] Zhao Q., J. Jiang, 1995. Robust SVC Controller Design for Improving Power System Damping, *IEEE Trans. Power Deliv.*, 10(4): 1927-1932.
- [10] Parniani M., M.R. Iravani, 1998. Optimal Robust Control Design of SVC, *IEEE Proc.-C*, 125(3): 301-307.
- [11] Farsangi M.M., Y.H. Song, Y.Z. Sun, 2000. supplementary control design of svc and statcom using H_∞ optimal robust control, *International Conference Electric Utility Deregulation and Restructuring and Power Technologies, DRPT 2000*, City University London, UK. pp: 355-360.
- [12] Farsangi M.M., Y.H. Song, W.L. Fang and X.F. Wang, 2002. Robust FACTS Control Design Using the H_∞ Loop-Shaping Method, *IEEE Proc.-C*, 149(3): 352-358.
- [13] Nabavi A., M.R. Iravani, 1996. Steady-state and dynamic models of UPFC for power sys. studies, *IEEE Trans. Power Deliv.*, 11(4): 1937-43.
- [14] Wang H.F., 1999. Damping function of UPFC, *IEEE Proc.-C*, Vol. 146, No. 1: 81-87.
- [15] Wang H.F., 1999. Application of modeling UPFC into multi-machine power systems, *IEEE Proc.-C*, 146(3): 306-312.
- [16] Skogestad S. and I. Postlethwaite, 1996. *Multivariable Feedback Control*, John Wiley.
- [17] Zhou K., J.C. Doyle, K. Glover, 1996. *Robust and Optimal Control*, Prentice-Hall, Inc.
- [18] YU Y.N., 1983. *Electric Power System Dynamics*, Academic Press, Inc., London.
- [19] Eldamaty A.A., S.O. Faried, S. Aboreshaid, 2005. Damping PSO Using a Fuzzy Logic Based UPFC, *IEEE CCECE/CCGEI*, 1: 1950-1953.
- [20] Randy L.H., E.H. Sue, 2004, *Practical Genetic Algorithms*, John Wiley & Sons, Second Edition, MATLAB Software, The Mathworks, Inc. 2006